Fluorescence Decay Kinetics of the Tryptophyl Residues of Myoglobin: Effect of Heme Ligation and Evidence for Discrete Lifetime Components†

K. J. Willis,‡ A. G. Szabo,*,‡ M. Zuker,‡ J. M. Ridgeway,‡ and B. Alpert§

Division of Biological Sciences, National Research Council of Canada, Ottawa, Ontario, Canada K1A 0R6, and Laboratoire de Biologie Physico-Chimique, Université de Paris VII, 75251 Paris, France

Received November 7, 1989; Revised Manuscript Received January 19, 1990

ABSTRACT: The fluorescence decay kinetics of the tryptophyl residues of sperm whale and yellowfin tuna myoglobin have been determined by using time-correlated single photon counting, with picosecond resolution. Purification by HPLC techniques resulted in the isolation of samples that exclusively displayed picosecond decay kinetics. Lifetimes of 24.4 ps for Trp^{14} and 122.0 ps for Trp^{7} were found for oxy sperm whale myoglobin (pH 7), which agree with theoretical predictions [Hochstrasser, R. M., & Negus, D. K. (1984) *Proc. Natl. Acad. Sci. U.S.A. 81*, 4399-4403]. The effects of ligand binding and pH on the decay kinetics were investigated, and the results were shown to be consistent with the known crystal structures. Data for the met form of sperm whale myoglobin were analyzed both in terms of a sum of discrete exponential components and as a continuous γ distribution of exponential decays. The results were not found to support the existence of multiple, structurally distinct conformation states in myoglobin.

The intrinsic fluorescence emission of proteins has proved to be a useful probe of protein structure, function, and dynamics (Beechem & Brand, 1985). Heme proteins, and their reaction with ligands, have been the subject of intense investigation for a number of years. However, the application of fluorescence spectroscopy to the study of heme proteins has been limited by the extremely low quantum yield of their tryptophyl emission.

The low tryptophyl quantum yield results from energy transfer to the heme moiety (Bücher & Kaspers, 1946; Weber & Teale, 1959). On the basis of energy-transfer calculations, Hochstrasser and Negus (1984) have predicted fluorescence lifetimes of ca. 30 ps and ca. 120 ps for Trp^{14} and Trp^{7} of sperm whale myoglobin, respectively. There have been several attempts to measure these decay kinetics (Hochstrasser & Negus, 1984; Janes et al., 1987; Bismuto et al., 1989); however, there is little agreement in the reported lifetimes and their relative contributions to the total fluorescence. In addition to picosecond decay components, nanosecond lifetimes were also reported. The origin of the nanosecond fluorescence lifetimes is uncertain. They may arise from non heme protein impurities or from structurally altered heme proteins with a reduced energy-transfer efficiency (Szabo et al., 1989).

In a study of sperm whale myoglobin (met)[1] by frequency domain fluorometry (Bismuto et al., 1989), the data were modeled with a continuous distribution of exponential decays. The resulting distribution was broad, extending over a time scale from a few picoseconds to several nanoseconds. The broad distribution was interpreted as evidence for the existence of multiple different conformational states in sperm whale myoglobin.

Energy-transfer and trajectory calculations (Hochstrasser & Negus, 1984; Janes et al., 1987) suggested that it was unlikely that native heme proteins could adopt a conformation which would result in nanosecond tryptophyl fluorescence lifetimes. Also, in a related study (Szabo et al., 1989), it was reported that human hemoglobin, purified by HPLC methods, exclusively displayed picosecond decay kinetics.

In this contribution, we present the results of time-correlated single photon counting experiments on sperm whale and yellowfin tuna myoglobins purified by HPLC. In sperm whale myoglobin, the effects of ligation state and pH on the tryptophyl fluorescence decay kinetics have been investigated. The data for the met form have been analyzed both in terms of a sum of discrete exponential components and as a continuous distribution of lifetimes. The results suggest that a simple two-component model is appropriate for the fluorescence decay of sperm whale myoglobin, in which the exclusively picosecond decay kinetics are subtly sensitive to the heme ligation state and pH-induced structural changes.

Experimental Procedures

Myoglobin (met) from sperm whale (*Physeter catodon*) and yellowfin tuna (*Thunnus albacares*) was prepared according to Fosmire and Brown (1976). Samples were further purified by nonideal size-exclusion HPLC on a Biosil TSK-125 column (600 × 7.5 mm; Bio-Rad) under isocratic elution with 0.01 M pH 7.0 phosphate buffer (Kopaciewicz & Regnier, 1982). SW Mb from two sources (Sigma and Fluka) was used and gave identical results.

Ferric SW Mb derivatives were prepared from the HPLC-purified met form by titration with the appropriate ligand. Ligation was monitored by spectrophotometry. Ferrous SW Mb derivatives were prepared as follows. SW Mb (met) in 0.01 M pH 7 phosphate buffer was reduced by addition of a small stoichiometric excess of dithionite in vacuo. Carbon monoxide was then introduced, and the sample was chromatographed as described above. During HPLC, the carbon monoxide was exchanged for oxygen (present in the buffer).

† Issued as NRCC Publication No. 31501. Financial assistance for B.A. was provided by the France-Canada exchange program. M.Z. is a fellow of the Canadian Institute for Advanced Research.

* Correspondence should be addressed to this author.

‡ National Research Council of Canada.

§ Université de Paris VII.

[1] Abbreviations: SW Mb, sperm whale myoglobin; met, ferric form; CN, cyanide derivative of the ferric form; N_3, azide derivative of the ferric form; O_2, oxy derivative of the ferrous form; CO, carbonyl derivative of the ferrous form; deoxy, unliganded ferrous form; YFT Mb, yellowfin tuna myoglobin; SVR, serial variance ratio.

0006-2960/90/0429-5270$02.50/0 Published 1990 by the American Chemical Society

The resulting oxymyoglobin was free from the met form. Deoxygenation of the MbO_2 was achieved by repetitive aspiration of a vessel to which a cell suitable for spectrophotometric measurements was attached. Nitrogen (or carbon monoxide to form MbCO) was then introduced.

The time-resolved fluorescence measurements were performed using time-correlated single photon counting with laser/microchannel plate instrumentation described in detail elsewhere (Willis & Szabo, 1989). The excitation wavelength was 295 nm, and emission was detected after passing through a polarizer set at 55° to the vertical, at 320 nm with a band-pass of 4 nm. The channel width was 1.0 ps, and data were collected in 1024 channels. An instrument response function was determined from the Raman scattering of D_2O at 320 nm (full width at half-maximum 60 ps). Each decay curve typically contained 3×10^5 total counts and required 5–10 min of data collection. A "no protein" blank was measured for each sample, for the same accumulation time, and the blank counts were subtracted from the sample decay curve. Measurements were conducted with a protein concentration of 1×10^{-5} M. Data for SW Mb (met) at pH 8.4 were collected to high precision (i.e., a large number of total counts). To increase the data collection rate, a band-pass of 8 nm was used, and the protein concentration was doubled to 2×10^{-5} M. To maintain the optical density, 0.5-cm cells were used.

The function describing the fluorescence intensity decay following δ-function excitation is assumed to be of the form

$$I(\lambda,t) = \int_0^\infty f(\lambda,k)e^{-kt}\,dk \quad (1)$$

where $k = 1/\tau$ and τ is a decay time. The kernel $f(\lambda,k)$ is the density that describes the distribution of reciprocal lifetimes. In the discrete exponential model:

$$f(\lambda,k) = \sum_{i=1}^{m} c_i(\lambda)\delta_{k_i} \quad (2)$$

so that

$$I(\lambda,t) = \sum_{i=1}^{m} c_i(\lambda)e^{-k_i t} \quad (3)$$

for m distinct lifetimes $1/k_1, 1/k_2, \ldots, 1/k_m$. Data were also analyzed assuming the function $f(\lambda,k)$ to be a sum of γ probability densities:

$$f(\lambda,k) = \sum_{i=1}^{m} c_i(\lambda)\alpha_i^{\nu_i}k^{\nu_i-1}e^{-\alpha_i k}/\Gamma(\nu_i) \quad (4)$$

The γ density $g_{\alpha,\nu}(k)$ defined by

$$g_{\alpha,\nu}(k) = \alpha^\nu k^{\nu-1}e^{-\alpha k}/\Gamma(\nu) \quad (5)$$

(Feller, 1971) has mean $E(k) = \nu/\alpha$ and variance $\sigma^2(k) = \nu/\alpha^2$. This leads to the equation for the decay profile:

$$I(\lambda,t) = \sum_{i=1}^{m} c_i(\lambda)/(1 + t/\alpha_i)^{\nu_i} \quad (6)$$

This can be rewritten by using the means, $k_i = E(k_i)$, and variances, $\sigma_i^2 = \sigma^2(k_i)$, of the reciprocal lifetimes directly:

$$I(\lambda,t) = \sum_{i=1}^{m} c_i(\lambda)\exp[-(k_i^2/\sigma_i^2)\ln(1 + \sigma_i^2 t/k_i)] \quad (7)$$

The $c_i(\lambda)$ terms are linear factors that describe the relative contributions of the m distributions.

Data were analyzed by a global (Knutson et al., 1983) nonlinear least-squares iterative convolution method based on the Marquardt (1963) algorithm. Adequacy of the fit of the model was judged by inspection of the plots of weighted residuals and of the statistical parameters χ^2 [the reduced χ^2 (Bevington, 1969)] and SVR [the serial variance ratio (Durbin & Watson, 1971)].

Results

HPLC. Nonideal size-exclusion chromatography of the commercial SW Mb (met) resulted in a chromatogram similar to that described by Kopaciewicz and Regnier (1982) for horse heart myoglobin. Purification of the commercial material by standard procedures prior to HPLC reduced the contribution of the minor peaks from ca. 30% to ca. 5% (based on the integrated absorption at 280 nm). Commercial samples could be purified in a single step if necessary. Similar results were obtained for YFT Mb (met).

The HPLC method was convenient and rapid; typically 200 μL of a 0.4 mM stock solution of myoglobin gave, in 30 min, 1 mL of approximately 40 μM purified protein which after suitable dilution was used immediately. A fresh preparation was used for each experiment (except in the case of deoxy and carbonyl SW Mb, which were prepared from the oxy form).

It is important to note that the SW MbO_2, produced by the method we have described, is free of the met form and stable for at least a day at 5 °C. The procedure avoids exposing the protein to dithionite in the presence of oxygen, which can result in side reactions (Dalziel & O'Brien, 1957).

Time-Resolved Fluorescence. Commercial samples of SW Mb (met) displayed multiexponential decay kinetics with components in the picosecond and nanosecond time ranges. Purification of the myoglobins by HPLC reduced the contribution of nanosecond fluorescence lifetime components to a level where they were not detected in the time-correlated single photon counting experiment. For comparison, under identical experimental conditions, the commercial (Fluka) SW Mb (met) showed a fractional fluorescence for nanosecond lifetime components of 0.25.

The results of time-resolved fluorescence measurements on myoglobins are summarized in Table I. The decay kinetics of HPLC-purified YFT Mb (met) were found to be single exponential with a lifetime of 33 ps. Under all conditions studied, a two-component discrete exponential model gave an excellent fit to the data for HPLC-purified SW Mb. The relative contributions of the two picosecond lifetime components were approximately equal in all cases (mean $c_1 = 0.45$, $c_2 = 0.55$; standard deviation 0.04).

The decay kinetics of SW Mb (met) at pH 7.0 were studied as a function of emission wavelength. To avoid wavelength-dependent temporal distortions, Stokes Raman scattering of the 295-nm excitation was used to record the instrument response functions (Willis et al., 1990). Three solvents were used to cover the emission range of 305–360 nm: deuterioacetonitrile (scattering at 314 nm), deuterium oxide (scattering at 320 nm), and water (scattering at 330 nm). Global analysis of data from 10 emission wavelengths resulted in an excellent fit to two components ($\chi^2 = 1.06$, SVR = 1.87, Table I) with fractional fluorescences independent of wavelength. The emission maximum was 325 nm.

The decay kinetics of SW Mb were found to vary with ligation state and pH (Table I). A range of 18–28 ps for τ_1 and 102–126 ps for τ_2 was observed, and this clearly exceeds the maximum standard error of ±1 ps (which is also the estimated resolution of our instrument; Szabo et al., 1989). To test our ability to accurately recover the parameters from a single data set, simulated data were generated. A measured instrument response function was convolved with a biexponential decay ($\tau_1 = 25$ ps, $c_1 = 0.44$; $\tau_2 = 112$ ps, $c_2 = 0.56$), the total counts were normalized to 2×10^5 (1×10^3 counts in the peak), and Poisson noise was added. A two-component

Table I: Results of Discrete Component Global Analysis of Myoglobin Emission Decay[a]

protein	pH[b]	no. of data sets[c]	τ_1 (ps)[d,e]	τ_2 (ps)	χ^2	SVR
YFT Mb (met)	6.0	4	33.0 ± 0.2		1.08	1.91
SW Mb (met)[f]	7.0	10	21.5 ± 0.5	112.5 ± 0.3	1.06	1.87
SW Mb (met)[g]	8.4	7	20.0 ± 0.1	113.7 ± 0.1	1.27	1.73
SW Mb (met)	6.0	8	22.8 ± 0.7	102.5 ± 0.4	1.02	1.92
SW Mb CN	6.0	8	28.5 ± 0.8	113.2 ± 0.4	1.03	1.95
SW Mb CN	8.4	8	28.2 ± 0.8	123.2 ± 0.3	1.03	1.90
SW Mb N_3	6.0	8	27 ± 1	109.4 ± 0.5	1.02	1.96
SW Mb N_3	8.4	8	23.9 ± 0.8	119.5 ± 0.4	1.02	2.01
SW Mb O_2	7.0	5	24.4 ± 0.9	122.0 ± 0.5	1.04	1.83
SW Mb O_2	8.4	4	24 ± 1	126.0 ± 0.7	1.03	2.04
SW Mb CO	7.0	6	23.4 ± 0.7	125.4 ± 0.4	1.04	1.91
SW Mb (deoxy)	7.0	6	18.0 ± 0.6	105.8 ± 0.3	1.03	2.00

[a] The excitation wavelength was 295 nm, and emission was monitored at 320 nm (4-nm band-pass). Stokes Raman scattering at 320 nm from D_2O was used to determine the instrument response function (FWHM 60 ps). Data were collected at 1 ps/channel in 1024 channels. [b] Samples purified by HPLC; 1×10^{-5} M in 0.01 M phosphate buffer, pH 7.0, 0.1 M phosphate buffer, pH 6.0, or 0.1 M Tris–acetate buffer, pH 8.4, at 20 °C. [c] Number of data sets used in the global analysis; one data set comprises instrument response function, sample, and blank. Sample decays contained ca. 3×10^5 total counts. [d] Lifetimes are given with their standard errors as recovered from a given global data set. These errors are derived from the diagonal elements of the covariance matrix in the nonlinear least-squares analysis. [e] There were no significant differences in the fractional fluorescences (average $f_1 = 0.14$, $f_2 = 0.86$; SD = 0.01) and normalized preexponentials (average $c_1 = 0.45$, $c_2 = 0.55$; SD = 0.04). [f] Data were collected at 10 emission wavelengths in the range 305–360 nm, 295-nm excitation. [g] The data in this global data set were collected to high precision and are equivalent to a single data set of 6×10^7 total counts (2.6×10^5 counts in the peak). An 8-nm band-pass was used, centered at 317 nm.

Table II: Bimodal Continuous γ Distribution Analysis of Myoglobin Decay Data[a]

constrained value of σ_i[b]	τ_1 (ps)[c]	τ_2 (ps)	HW_1[d] (ps)	HW_2 (ps)	χ^2	SVR
$k_i^*/2$	7	80	1	33	2.88	0.34
$k_i^*/4$	14	100	3	26	1.54	1.20
$k_i^*/6$	17	106	3	20	1.33	1.58
$k_i^*/8$	18	109	2	15	1.29	1.69
$k_i^*/16$	20	113	1	8	1.27	1.74
$k_i^*/32$	20	113	1	4	1.27	1.73
biexponential fit[e]	20	114			1.27	1.73

[a] The myoglobin data were for SW Mb (met) at pH 8.4 (see Table I). Seven data sets were analyzed using a global method. The global data set was equivalent to a single data set with 2.6×10^5 counts in the peak channel. [b] In the analysis, the standard deviation of k_i was fixed at a given fraction of k_i^*; $k_i^* = 1/\tau_1$ and $k_2^* = 1/\tau_2$ where $\tau_1 = 20$ ps and $\tau_2 = 114$ ps, which are the lifetime values recovered by the biexponential (two discrete component) fit. All other parameters were unconstrained. [c] These are the mean lifetimes associated with each mode of the distribution. [d] The half-width at half-height of the distribution $HW_i = (2 \ln 2)^{1/2}\sigma_i/k_i^2$. [e] Included from Table I for comparison.

fit recovered the parameters with high precision ($\tau_1 = 25 \pm 2$ ps, $c_1 = 0.44$; $\tau_2 = 111 \pm 1$ ps, $c_2 = 0.56$; $\chi^2 = 0.962$, SVR = 1.98). It is important to note that the parameters listed in Table I result from global analysis of at least four data sets, each individual data set having ca. 3×10^5 total counts. As a further illustration of the relative accuracy of the parameter recovery, the data for SW Mb (met) at pH 8.4 were analyzed with the two lifetimes constrained to the values found for SW Mb (met) at pH 6.0. The result was a fit of reduced quality ($\chi^2 = 1.3$, SVR = 1.48), strongly suggesting that the difference of 10 ps in the value of τ_2 between the two pHs is significant.

Distribution Model. The discrete exponential model was fitted to the data to determine the kinetic parameters presented above. Data which are well described by a two-component discrete exponential model may also be equally well described by a model in which it is assumed that there is a continuous distribution of exponential decays (James & Ware, 1985; Bayley & Martin, 1989). High-precision data are required if one is to attempt to distinguish between these two models. For single photon counting, data precision increases as $N_i^{1/2}$, where N_i is the number of counts in channel i (O'Conner & Phillips, 1984).

Seven data sets were collected for SW Mb (met) (at pH 8.4) and were analyzed simultaneously using a global method (Knutson et al., 1983). The global data set contained 6×10^7 total counts, equivalent to a single data set with 2.6×10^5 counts in the peak channel. When we attempted to fit these data using the superposition of two γ distributions (henceforth referred to as a bimodal distribution fit), the nonlinear least-squares minimization failed to converge. The mean lifetimes of the two distributions were then "fixed" to the values resulting from discrete exponential analysis (given in Table I) of these data, and again the analysis failed to converge. This suggested that the quality of the fit was relatively insensitive to small variations in the standard deviations (σ_i; related to the width, see Table II) of the two distributions. Similar observations have been made by James and Ware (1985) and Bayley and Martin (1989).

By "fixing" the standard deviations of the bimodal model's two distributions, we were able to investigate the effect of various standard deviations of the distributions, on the quality of the fit, and on the values of the recovered parameters. The results are presented in Table II. The form of the distribution when σ_i is constrained at $k_i^*/8$ (see Table II) is illustrated in Figure 1; as we will discuss later, this distribution represents an upper limit for the widths of the bimodal distributions which are consistent with our data.

Discussion

Multiexponential fluorescence decay kinetics are frequently observed for protein tryptophyl residues (Beechem & Brand, 1985) reflecting perhaps some degeneracy in the indole microenvironment. Janes et al. (1987) have suggested that in the case of heme proteins each tryptophyl residue might be expected to display single-exponential decay kinetics, as the rate of deactivation of the excited state by energy transfer should greatly exceed all other competing processes. The observed fluorescence lifetimes will therefore be determined primarily by the rate of energy transfer.

Sperm whale myoglobin contains two tryptophyl residues (Edmundson, 1965), Trp^7 and Trp^{14}. An examination of the X-ray structure indicates that Trp^{14} is 15.0 Å from the heme

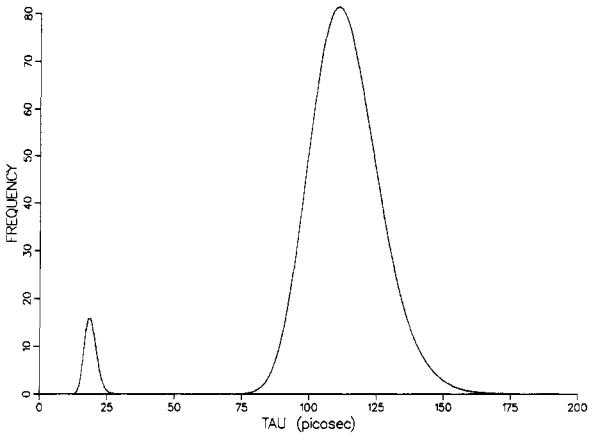

FIGURE 1: Bimodal continuous γ distribution of exponential decays for sperm whale myoglobin (met) at pH 8.4. Our data are equally consistent with all bimodal γ distributions (centered at ca. 20 and ca. 110 ps) with widths less than or equal to that illustrated in the figure (including two discrete exponentials).

with the plane of the indole ring oriented approximately parallel to that of the heme. Trp^7 is oriented with the plane of the indole ring orthogonal to the heme, and the separation is 21.5 Å. As a result of energy-transfer calculations, based on the X-ray structure, Hochstrasser and Negus (1984) predicted fluorescence lifetimes of 31 ps (Trp^{14}) and 125 ps (Trp^7) for deoxy SW Mb and 41 ps (Trp^{14}) and 121 ps (Trp^7) for carbonyl SW Mb. A single-exponential lifetime of 30–40 ps was predicted by them for the single tryptophan (Trp^{14}) of YFT Mb. They were able to detect approximately these values in the presence of nanosecond lifetime components by utilizing the high time resolution and narrow time window of a streak camera. Our results are in reasonable agreement with the predicted values.

The energy-transfer calculations were unable to account for the minor contribution from nanosecond lifetime components reported in previous studies of intact myoglobin (Hochstrasser & Negus, 1984; Janes et al., 1987; Bismuto et al., 1989). We find that while these nanosecond components are observed for samples of the commercial material, they are not detected following HPLC purification. As the tryptophyl emission from intact myoglobin is extremely weak, the fluorescence properties observed may be dominated by even trace amounts of fluorescent contaminants. We did not attempt to characterize the nanosecond fluorescence present prior to HPLC purification. The nanosecond fluorescence may arise from non-myoglobin impurities or from structurally altered myoglobins. It has recently been reported that the nanosecond lifetime components can also be eliminated from hemoglobin samples by HPLC purification techniques (Szabo et al., 1989).

According to energy-transfer theory (Förster, 1965), we might expect to see a change in the observed fluorescence lifetimes on ligation of the heme, if this is accompanied by a change in the relative separation or orientation of the tryptophyl and heme moieties, or if their spectral distributions alter. Trp^7 and Trp^{14} are the 5th and 12th residues of the A helix of myoglobin. Both are located in surface crevices with similar solvent exposure, which is consistent with our finding that the spectra associated with the two decay components were identical (maxima at ca. 325 nm). Crystal structures of the met (Tanko, 1977a), deoxy (Tanko, 1977b), carbonmonoxy (Norvell et al., 1975), and oxy forms of myoglobin (Phillips, 1978) indicate that the A helix has no direct contact with the heme and that there is little movement in the A helix relative to the heme. For example, the rms difference between the deoxy and met forms for the A helix is 0.14 Å (Tanko, 1977b).

The crystal structures also show that there is no change in heme orientation on ligand binding. Polarized ultraviolet absorption measurements of single myoglobin crystals can also provide information on the heme orientation. Since the heme Soret band is in-plane polarized, tilting of the heme will alter the polarization ratios along the different crystal axes. These optical data also indicate that there is little change in the heme orientation (Eaton & Hofrichter, 1981). Changes in the orientation of the tryptophyl residues are not expected since the A helix is largely unaffected by ligand binding. Furthermore, it has been calculated that except for a small fraction of the possible orientations of the tryptophyl residue's transition moments, the energy-transfer rate in myoglobin is relatively insensitive to this parameter (Hochstrasser & Negus, 1984).

The above discussion suggests that the changes in the tryptophyl lifetimes which we have observed with ligation of the heme are mainly due to different degrees of overlap between the tryptophyl emission and the heme absorption spectra (quantified by the overlap integral; Förster, 1965). Our results indicate that the emission spectra of the two tryptophyl residues are closely similar and show little change with heme ligation. However, significant changes in the absorption spectra of myoglobin are known to occur on ligation (Hardman et al., 1966; Hanania et al., 1966). We determined that absorption spectral changes at pH 7, with heme ligand, reduced the overlap integral (Förster, 1965) to 82% (carbonyl), 88% (met), and 91% (oxy) of the values for deoxymyoglobin. Using the observed lifetime values for deoxymyoglobin at pH 7, and the relative overlap integral changes, we can predict the lifetime values of the liganded forms [by using the equations given by Hochstrasser and Negus (1984)] as follows (observed values are given in parentheses): SW Mb CO, 22 ps (23) and 129 ps (125); SW Mb (met), 20 ps (21) and 120 ps (112); SW Mb O_2, 20 ps (24) and 116 ps (112). The spectral differences account for the majority of the observed changes in tryptophyl lifetimes. Since both tryptophans are close to the surface of the protein, the minor discrepancy between predicted and observed results may indicate that the equilibrium position and orientation of the tryptophyl residues differ by a small amount in the crystal and solution. Trite calculation shows that a change in the heme to Trp^7 separation of just 0.2 Å could result in a 6-ps increase in the Trp^7 lifetime (based on a lifetime of 106 ps and a donor–acceptor separation of 21.5 Å).

In metmyoglobin, the sixth coordination position of the iron atom is occupied by H_2O or by OH^- (Stryer et al., 1964). Comparing SW Mb^+-H_2O (at pH 6.0) with SW Mb^+-OH^- (at pH 8.4), we found a 10-ps increase in the fluorescence lifetime of Trp^7. This 10-ps increase with pH was also observed for the met derivatives in which cyanide or azide occupied the sixth coordination position. It is unlikely that this is due to changes in the overlap integral since the spectra of the cyanide and azide derivatives are pH-insensitive (Hanania et al., 1966; Antonini & Brunori, 1971). Underivatized metmyoglobin does show pH-dependent absorption spectra, but the differences in the spectral overlap region (ca. 300–400 nm) are small (Hanania et al., 1966). X-ray crystallographic investigations of the neutral and alkaline SW Mb (met) found several structural differences associated with the deprotonation of imidazole groups of histidine residues (Schoenborn, 1969). No significant change in the relative positions and orientations of the A helix and heme moiety was detected. There was, however, some evidence for a specific effect at Trp^7, namely, the loss of a hydrogen bond with Glu^6. Such a change could,

in principle, account for the observed lifetime increase. The lifetime differences between the different met derivatives at a given pH can probably be accounted for by overlap integral changes, as they have different absorption spectra (Hanania et al., 1966; Antonini & Brunori, 1971) but closely similar crystal structures (Stryer et al., 1964; Bretcher, 1968).

It is interesting to compare the fluorescence lifetime assigned to Trp^{14} of SW Mb (met), 23 ps, with the value of 33 ps observed for YFT Mb (met) (at pH 6). YFT Mb has only one tryptophan, Trp^{14}, and the X-ray structure is similar to that of SW Mb (Lattman et al., 1971). Comparing the X-ray coordinates for SW Mb (met) at 2-Å resolution (Tanko, 1977a) and YFT Mb (met) at 1.7-Å resolution (G. I. Birnbaum, personal communication), we find that the heme to Trp^{14} separation is 0.6 Å greater in YFT Mb. The orientation factors, calculated from the X-ray coordinates by using the formulations given by Hochstrasser and Negus (1984), are identical. As the overlap integrals are similar for the two proteins, we would expect the increased heme to Trp^{14} separation to result in a lifetime of 29 ps for YFT Mb, which is approximately what is observed.

In the preceding discussion, we have interpreted our results in terms of a biexponential model in which each tryptophyl residue was assigned a discrete lifetime. It has been shown that at the commonly used levels of data precision, data which yield excellent fit statistics to a two-component discrete exponential model can also be equally well described by a model in which a continuous distribution of exponential decays is assumed (James & Ware, 1985; Bayley & Martin, 1989). Despite its increased complexity, the distribution model is attractive since the extra parameter, the width of the distribution, may have physical significance in terms of protein dynamics and structure. A distribution of donor–acceptor separations and relative orientations could arise in myoglobin from dynamic fluctuations of the protein on the time scale of the experiment (Karplus & McCammon, 1981; Somogyi et al., 1984) or from the existence of multiple different conformational states (Frauenfelder et al., 1988; Alcala et al., 1987).

Bismuto et al. (1989) have examined the tryptophyl fluorescence decay kinetics of SW Mb by frequency domain fluorometry. They found that for the met form at pH 7, data were best fitted by a sum of three exponentials with lifetimes of 80 ps, 1 ns, and 8 ns. They also reported that a continuous distribution model, using the superposition of three Lorentzian distributions, gave an improved fit to the data. The resulting distribution was very broad, with significant density over the range 0–7.5 ns. This broad distribution was interpreted in terms of a large number of conformational states which were unable to interconvert on the time scale of the experiment. The width of the distribution is surprising since, as we noted earlier, it is unlikely that myoglobin could adopt a conformation which would lead to fluorescence lifetimes on the nanosecond time scale (Hochstrasser & Negus, 1984; Janes et al., 1987).

We collected data for the met form of SW Mb, at pH 8.4, to a large number of counts per channel and analyzed the data using both a two-component discrete exponential model and a bimodal γ distribution model. The γ distribution is characterized by a mean and standard deviation and is similar to a Gaussian distribution, when the ratio of the standard deviation to the mean is small. A γ distribution has the advantage that since the distribution starts at zero (rather than negative infinity in the case of Gaussian and Lorentzian distributions) artificial truncation is not necessary.

When the ratio of the standard deviation to the mean was made very small (corresponding to a narrow distribution), the quality of the bimodal γ distribution fit to the data equaled, but did not exceed, that given by a two-component discrete exponential model. The mean lifetimes and preexponential factors for the distribution fit were identical with the corresponding parameters obtained from the two-component discrete exponential model. The quality of the fit and the recovered parameters were insensitive to small increases in the standard deviation of the distributions. Larger increases significantly reduced the quality of the fits, and the recovered mean lifetimes decreased. This approach allowed us to empirically determine the maximum standard deviations (and hence widths, see Table II) that could be accommodated before there was a significant decrease in the quality of the fit, as judged by the statistical parameters. The form of the distribution which resulted when the standard deviations were constrained to these "maximum" values is shown in Figure 1. It is important to stress that narrower bimodal distributions, with the same means, gave identical fit statistics and also that the quality of the fit for the distribution model did not exceed that given by the two-component discrete exponential model.

The distribution of exponential decays shown in Figure 1 is narrow, with full widths at half-maximum for the two modes of 4 and 30 ps. This strongly suggests that multiple conformations of the A helix, relative to the heme, if present, are structurally highly homogeneous. For example, lifetime changes of the order of ±15 ps for Trp^7 could easily be caused by changes in the Trp to heme separation of the order of 1 Å or less or by rotations of a few degrees about the β–γ bond (Negus & Hochstrasser, 1984). A small number of conformations, each with different tryptophan lifetimes, dependent on their separation and orientation with respect to heme, would give rise to nonexponential decay kinetics (Henry & Hochstrasser, 1987) which we do not observe for myoglobin. Narrow distributions would be expected if the protein conformations were rapidly interconverting on the time scale of the experiment. It is unlikely that at 20 °C there is significant interconversion of conformers with different tryptophyl fluorescence lifetimes on the tens of picosecond time scale. Molecular dynamics simulations suggest that the tryptophan side chains of myoglobin did not undergo large reorientations on the picosecond time scale (Henry & Hochstrasser, 1987). Our results do not exclude the presence of conformational substates in which the spatial relationship of the A helix, relative to the heme, is unchanged. Indeed, as we have discussed earlier, the structural changes which accompany ligand binding almost meet this criterion.

It may be possible to set further limits on the widths of the bimodal distribution if more precise data cound be collected. The global data set used in the distribution analysis contained ca. 6×10^7 total counts and because of the weak fluorescence of myoglobin required some 4 h of data collection. Maintaining picosecond resolution over a period of several hours was a severe test of instrumental stability and is reflected in the slightly reduced quality of the fits with both discrete exponential *and* distribution models. The reduced quality of the fit is also partly a consequence of the larger band-pass used (8 nm as opposed to 4 nm for other data) which increases the temporal distortion of the detection system. It is important to note that other methods which attempt to distinguish between discrete exponential and distribution models, such as the exponential series (James et al., 1987) and maximum entropy (Livesey & Brochon, 1987) methods, also require high data precision.

We have shown that the fluorescence decay kinetics of tryptophyl residues in myoglobin can yield useful structural

information. Unfortunately, their natural location on the A helix limits their ability to probe ligation-induced structural changes. Clearly, it would be interesting to examine mutant proteins with tryptophyl residues located in other, more mobile, regions of the protein. It is important to note, however, that locations close to the heme moiety, for example, on the F helix, would result in tryptophyl fluorescence lifetimes of only a few picoseconds.

ACKNOWLEDGMENTS

The technical assistance of D. T. Krajcarski is greatfully acknowledged. Preliminary purification of the myoglobin samples was performed by Dr. T. M. Stepanik, to whom we are indebted. We also thank Dr. G. I. Birnbaum for allowing us access to the X-ray coordinates of YFT Mb prior to publication.

Registry No. CN, 57-12-5; N_3, 14343-69-2; O_2, 7782-44-7; CO, 630-08-0.

REFERENCES

Alcala, J. R., Gratton, E., & Prendergast, F. G. (1987) *Biophys. J. 51*, 597.

Antonini, E., & Brunori, M. (1971) *Hemoglobin and Myoglobin in their Interactions with Ligands*, p 49, North-Holland, Amsterdam.

Bayley, P., & Martin, S. (1989) in *Fluorescent Biomolecules* (Jameson, D. M., & Reinhart, G. D., Eds.) p 389, Plenum Press, New York.

Beechem, J. M., & Brand, L. (1985) *Annu. Rev. Biochem. 54*, 43.

Bevington, P. B. (1969) *Data reduction and error analysis for the physical sciences*, Chapter II, McGraw-Hill, New York.

Bismuto, E., Irace, G., & Gratton, E. (1989) *Biochemistry 28*, 1508.

Bretcher, P. A. (1968) Ph.D. Dissertation, Cambridge University.

Bücher, T., & Kaspers, J. (1946) *Naturwissenschaften 33*, 93.

Dalziel, K., & O'Brien, J. R. P. (1957) *Biochem. J. 67*, 119.

Durbin, J., & Watson, G. S. (1971) *Biometrika 58*, 1.

Eaton, W. A., & Hofrichter, J. (1981) *Methods Enzymol. 76*, 175.

Edmundson, A. B. (1965) *Nature 205*, 883.

Feller, W. (1971) *An Introduction to Probability Theory and Its Applications*, 2nd ed., Vol. II, p 47, Wiley, New York.

Förster, Th. (1965) in *Modern Quantum Chemistry* (Sinanoglu, O., Ed.) Vol. 3, p 93, Academic Press, New York.

Fosmire, G. J., & Brown, W. D. (1976) *Comp. Biochem. Physiol., B: Comp. Biochem. 55B*, 293.

Frauenfelder, H., Parak, F., & Young, R. D. (1988) *Annu. Rev. Biophys. Chem. 17*, 451.

Hanania, G. I. H., Yeghiayan, A., & Cameron, B. F. (1966) *Biochem. J. 98*, 189.

Hardman, K. D., Eylar, E. H., Ray, D. K., Banaszak, L. J., & Gurd, F. R. N. (1966) *J. Biol. Chem. 241*, 432.

Henry, E. R., & Hochstrasser, R. M. (1987) *Proc. Natl. Acad. Sci. U.S.A. 84*, 6142.

Hochstrasser, R. M., & Negus, D. K. (1984) *Proc. Natl. Acad. Sci. U.S.A. 81*, 4399.

James, D. R., & Ware, W. R. (1985) *Chem. Phys. Lett. 120*, 455.

James, D. R., Turnbull, J. R., Wagner, B. D., Ware, W. R., & Petersen, N. O. (1987) *Biochemistry 26*, 6272.

Janes, S. M., Holtom, G., Ascenzi, P., Brunori, M., & Hochstrasser, R. M. (1987) *Biophys. J. 51*, 653.

Karplus, M., & McCammon, J. A. (1981) *CRC Crit. Rev. Biochem. 9*, 293.

Knutson, J. R., Beechem, J. M., & Brand, L. (1983) *Chem. Phys. Lett. 102*, 501.

Kopaciewicz, W., & Regnier, F. E. (1982) *International Symposium on HPLC Proteins and Peptides*, 1981, Paper 127, Washington, D.C.

Lattman, F. E., Nockolds, C. E., Kretsinger, R. H., & Love, W. E. (1971) *J. Mol. Biol. 60*, 271.

Livesey, A. K., & Brochon, J. C. (1987) *Biophys. J. 52*, 693.

Marquardt, D. W. (1963) *J. Soc. Ind. Appl. Math. 11*, 431.

Negus, D. K., & Hochstrasser, R. M. (1984) *J. Lumin. 31*, 3.

Norvell, J. C., Nunes, A. C., & Schoenborn, B. P. (1975) *Science 190*, 568.

O'Connor, D. V., & Phillips, D. (1984) *Time-correlated Single Photon Counting*, Academic Press, London.

Phillips, S. E. V. (1978) *Nature 273*, 247.

Schoenborn, B. P. (1969) *J. Mol. Biol. 45*, 297.

Somogyi, B., Matko, K., Papp, S., Hevessy, J., Welch, G. R., & Damjanovich, S. (1984) *Biochemistry 23*, 3403.

Stryer, L., Kendrew, J. C., & Watson, H. C. (1964) *J. Mol. Biol. 8*, 96.

Szabo, A. G., Willis, K. J., Krajcarski, D. T., & Alpert, B. (1989) *Chem. Phys. Lett. 163*, 565.

Tanko, T. (1977a) *J. Mol. Biol. 110*, 537.

Tanko, T. (1977b) *J. Mol. Biol. 110*, 569.

Weber, G., & Teale, F. W. J. (1959) *Discuss. Faraday Soc. 27*, 134.

Willis, K. J., & Szabo, A. G. (1989) *Biochemistry 28*, 4902.

Willis, K. J., Szabo, A. G., & Krajcarski, D. T. (1990) *Photochem. Photobiol. 51*, 375.